

Figure 4 depicts the fin effectiveness  $\phi$  based on an isothermal fin for both the complete and simple models. The effectiveness  $\phi$  decreases as  $N_\infty$  and  $Pr$  increase since the fin becomes more and more nonisothermal due to decreased fin conductance ( $K_f r_f$ ) and/or increased convective effects. Though the difference in  $\phi$  for the two models is small, it may be pointed out that the higher the values of  $N_\infty$  and  $Pr$  the more conservative the simple model gets. These results are for  $R_0 = 4$ . We know [9] that the fin temperature becomes less uniform as  $R_0$  decreases due to lower fin conductance. Thus, the fin effectiveness will decrease with decreasing  $R_0$ . The overall heat transfer rate  $Q_N$  from the fin can be easily calculated from Fig. 4 and Table 1, and is therefore not presented separately.

## 6. CONCLUSIONS

A numerical solution of the coupled fin conduction equation and the laminar, forced convective boundary layer equations for a cylindrical fin has been carried out. The effects of Prandtl number and the conduction-convection parameter on the heat transfer characteristics have been studied. It has been found that the dimensionless average heat transfer coefficient for an isothermal cylindrical fin is nearly proportional to  $Pr^{0.3}$ . While the simple model predicts the fin effectiveness and the overall heat transfer rate from the fin within tolerable accuracy over the entire range of  $Pr$  values, its predictions of local heat flux and fin temperature are in substantial error.

**Acknowledgements**—The computing facility availed at the Indira Gandhi Centre for Atomic Research, Kalpakkam, India, is gratefully acknowledged. The first author would also like to acknowledge the support from The Ohio State University during his sabbatical.

## REFERENCES

1. E. M. Sparrow and M. K. Chyu, Conjugate forced con-

2. E. M. Sparrow and S. Acharya, A natural convection fin with a solution-determined nonmonotonically varying heat transfer coefficient, *ASME J. Heat Transfer* **103**, 218-225 (1981).
3. B. Sundén, Conjugate mixed convection heat transfer from a vertical rectangular fin, *Int. Commun. Heat Mass Transfer* **10**, 267-276 (1983).
4. B. Sundén, A numerical investigation of coupled conduction-mixed convection for rectangular fins, *Proc. 3rd Int. Conf. Numer. Meth. in Laminar and Turbulent Flow*, Aug. 1983, Seattle, pp. 809-819. Pineridge Press, Swansea (1983).
5. V. K. Garg and K. Velusamy, Heat transfer characteristics for a plate fin, *ASME J. Heat Transfer* **108**, 224-226 (1986).
6. B. Sundén, The effect of Prandtl number on conjugate heat transfer from rectangular fins, *Int. Commun. Heat Mass Transfer* **12**, 225-232 (1985).
7. M. J. Huang and C. K. Chen, Vertical circular pin with conjugated forced convection-conduction flow, *ASME J. Heat Transfer* **106**, 658-661 (1984).
8. M. J. Huang, C. K. Chen and J. W. Cleaver, Vertical circular pin with conjugated natural convection-conduction flow, *ASME J. Heat Transfer* **107**, 242-245 (1985).
9. K. Velusamy and V. K. Garg, Heat transfer from a cylindrical fin in combined free-forced flow, *Int. J. Heat Fluid Flow* **9**(2), 233-240 (1988).
10. E. R. G. Eckert and R. M. Drake, *Analysis of Heat and Mass Transfer*. McGraw-Hill, Tokyo (1972).
11. R. W. Hornbeck, Numerical marching techniques for fluid flows with heat transfer, NASA SP-297, Washington, DC (1973).
12. H. S. Yu and E. M. Sparrow, Local nonsimilarity thermal boundary layer solutions, *ASME J. Heat Transfer* **93**, 328-334 (1971).

## Transient forced convection heat transfer from a circular cylinder in a saturated porous medium

SHIGEO KIMURA

Government Industrial Research Institute, Tohoku, 4-2-1 Nigatake, Sendai 983, Japan

(Received 22 March 1988 and in final form 23 June 1988)

### 1. INTRODUCTION

TRANSIENT heat transfer from a cylinder placed in a fluid-saturated porous medium is considered. It is assumed that the flows are perpendicular to the cylinder axis and the velocities are sufficiently large to neglect the buoyant force caused by temperature differences, but small enough to ensure the validity of Darcy's law. When the wall temperature of the cylinder is raised to  $T_w$  and maintained at that temperature thereafter, the thin thermal boundary layer is formed during a small time period. The thermal layer then grows with time until the radial thermal diffusion is eventually balanced with the cross convection. The associated steady-state problem was first considered by Cheng [1] with boundary layer approximations. The analysis has been recently extended by Kimura [2] to cylinders of elliptic cross

sections with integral methods. The forced convection from a cylinder has important applications in an area for shallow geothermal energy use and development. For instance a shallow aquifer, which is kept at a temperature of about 10°C during the winter time, is a possible heat source for house heating and other uses in cold regions. Development of heat extraction techniques from shallow aquifers with cylindrical heat exchangers, i.e. large heat pipes, requires knowledge on heat transfer described in the present problem.

### 2. MATHEMATICAL FORMULATION AND SOLUTION PROCEDURE

Nondimensionalized conservation equations for momentum and energy with the assumption of Darcy's law and

## NOMENCLATURE

<i>a</i>	radius of circular cylinder [m]
<i>c</i>	specific heat at constant pressure [J kg <sup>-1</sup> K <sup>-1</sup> ]
<i>H</i>	dimensionless constant to determine a computational domain, equation (7)
<i>k<sub>e</sub></i>	effective thermal conductivity [W m <sup>-1</sup> K <sup>-1</sup> ]
<i>Nu</i>	Nusselt number, $2\pi a q''/\Delta T k$
<i>Pe</i>	Peclet number, $Ua/\alpha$
<i>q''</i>	heat flux in a unit area [W m <sup>-2</sup> ]
<i>T</i>	temperature [K]
$\Delta T$	temperature difference, $T_w - T_\infty$ [K]
<i>U</i>	free stream velocity [m s <sup>-1</sup> ]
<i>W</i>	dimensionless constant to determine a computational domain, equation (7)
<i>x</i>	dimensionless horizontal coordinate
<i>y</i>	dimensionless vertical coordinate.

Greek symbols	
$\alpha$	effective thermal diffusivity defined by equation (5)
$\gamma$	Euler's constant in equation (8)
$\theta$	dimensionless temperature
$\rho$	fluid density
$\sigma$	heat capacity ratio defined by equation (3)
$\tau$	dimensionless time, $t\alpha/\sigma a^2$
$\phi$	porosity of porous matrix
$\psi$	dimensionless stream function.

## Subscripts

<i>2a</i>	characteristic length in defining Peclet number
<i>f</i>	thermal properties of fluid
<i>s</i>	thermal properties of solid matrix
<i>w</i>	conditions at cylinder wall
$\infty$	conditions at infinity.

thermodynamic equilibrium between a porous matrix and the saturated fluid are

$$\nabla^2 \psi = 0 \quad (1)$$

$$\frac{\partial \theta}{\partial \tau} + Pe \frac{\partial(\theta, \psi)}{\partial(x, y)} = \nabla^2 \theta. \quad (2)$$

The velocity, temperature, length and time are scaled by incoming free velocity  $U_\infty$ , temperature difference  $T_w - T_\infty$ , radius of the cylinder and diffusion time defined by  $\sigma a^2/\alpha$ , respectively. The continuity equation has been eliminated in a usual manner by introducing the stream function  $\psi$ . The Peclet number,  $Pe$ , is based on the cylinder radius.  $\sigma$  is the thermal capacity ratio of the saturated porous matrix to the saturated fluid as defined by equation (3).  $\alpha$  is the effective thermal diffusivity defined by the volume-averaged thermal conductivity divided by the thermal capacity of the saturated fluid as in equations (4) and (5)

$$\sigma = \frac{(\rho c)_f \phi + (1 - \phi)(\rho c)_s}{(\rho c)_f} \quad (3)$$

$$k_e = k_f \phi + (1 - \phi) k_s \quad (4)$$

$$\alpha = \frac{k_e}{(\rho c)_f} \quad (5)$$

where  $\phi$  is the porosity of the solid matrix and subscripts *s* and *f* indicate properties of the solid matrix and saturated fluid, respectively. Supposing a rectangular domain as shown in Fig. 1, the boundary conditions of equations (1) and (2)

are

$$\begin{aligned} \theta = 1, \quad \psi = 0 & \quad \text{on} \quad \sqrt{(x^2 + y^2)} = 1 \\ \theta = 0, \quad \psi = y & \quad \text{on} \quad x = -W \\ \theta_y = 0, \quad \psi = H & \quad \text{on} \quad y = H \\ \theta_x = 0, \quad \psi_x = 0 & \quad \text{on} \quad x = W. \end{aligned} \quad (6)$$

## 2.1. Small-time solution

In a small time after the temperature of the cylinder surface is raised, the thermal boundary layer is still thin and it may not feel the presence of the convecting flows [3, 4]. This assumption reduces the governing equations to a simple heat conduction equation. The solution in terms of Nusselt number is expressed by

$$Nu = \frac{2\pi a q''}{k_e \Delta T} = 2\pi \left\{ \frac{1}{\sqrt{\pi \tau}} + \frac{1}{2} - \frac{1}{2} \sqrt{\frac{\tau}{\pi}} + \frac{\tau}{8} - \dots \right\} \quad (7)$$

for a small  $\tau$  and

$$Nu = 4\pi \left\{ \frac{1}{\ln(4\tau) - 2\gamma} - \frac{\gamma}{\{\ln(4\tau) - 2\gamma\}^2} - \dots \right\} \quad (8)$$

for a large  $\tau$ , where  $\gamma = 0.57722 \dots$  [5].

## 2.2. Steady-state solution

As time elapses, the thermal layer grows steadily. The balance between the radial diffusion and the transverse convection in the energy equation will eventually lead to a steady state. Neglecting the time derivative in the energy equation and assuming the thermal boundary layer thickness is still small relative to the radius of the cylinder, the equation may be integrated once in the radial direction to yield an integral form of the energy conservation statement. The average Nusselt number for the steady state by integral solution [2] reads

$$Nu = 3.10 \sqrt{(Pe_{2a})}. \quad (9)$$

The above expression is accurate when  $Pe_{2a} > 3$ , where the subscript *2a* indicates the characteristic length used in the definition.

## 2.3. Numerical solution of complete governing equations

A full two-dimensional solution of equations (1) and (2) in terms of finite differences has been sought in order to bridge the two extremities; pure conduction and steady-state convection. The rectangular region of Fig. 1 is divided into a non-uniform grid network. Sufficiently fine grid spaces are

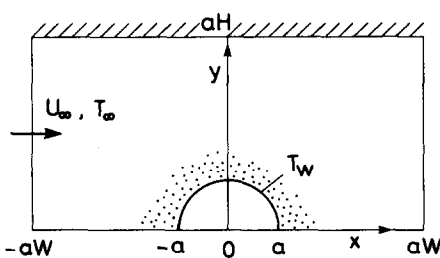


FIG. 1. Circular cylinder in a saturated porous matrix with uniform cross flows.

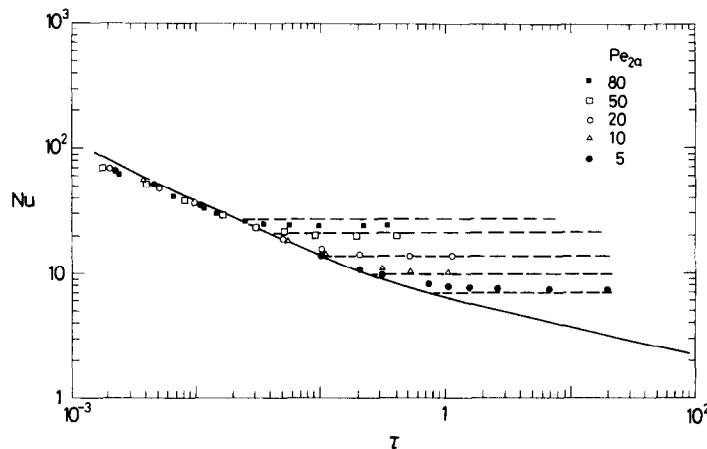


FIG. 2. Nusselt number during transient process. Solid and dashed lines are by pure conduction and by steady-state integral solution, respectively. Various symbols are due to numerical solution.

employed near the cylinder, while relatively coarse ones are used in the far field together with an apparent symmetry relative to the  $x$ -coordinate in order to save computer time. The size of the computational domain is controlled by assigning arbitrary large numbers on  $H$  and  $W$ . Care has been taken to ensure a large enough area not to affect the solution, particularly for small Peclet numbers.

### 3. RESULTS AND DISCUSSION

Heat transfer results obtained by the previous section are all assembled in Fig. 2. The Nusselt numbers are plotted as a function of non-dimensional time  $\tau$ , while the Peclet number based on cylinder diameter is used as a parameter. A solid line indicates the Nusselt number from the pure conduction solution (equations (7) and (8)). Dashed lines indicate the convective steady-state Nusselt numbers obtained from equation (9). Various symbols on the figure show the Nusselt numbers from the numerical solution. Numerical results, in general, agree well with the solid line for small values of  $\tau$  and with the dashed lines for large values of  $\tau$  at respective Peclet numbers. Steady decreases in Nusselt number along the solid line and the gradual deviations to approach to respective constant values are the common feature seen for all Peclet numbers in the transient process. The smooth transition from pure conduction to convective steady solution without passing through any oscillatory behavior, which is often observed in the transient solution of ordinary fluids, is one characteristic of the present problem. Insufficient resolution of the boundary layer in the numerical solution, however, under-estimates Nusselt numbers in the early stage of pure conduction ( $\tau < 5 \times 10^{-3}$ ) and in the convective steady state of large Peclet numbers. In both cases extremely thin boundary layers are expected. Figure 3 shows the temperature fields at three different  $\tau$ 's during the boundary layer development. The isotherms shown in a sequential manner clearly support the earlier view on the transient process. For example at  $\tau = 0.01$  all isotherms are nearly concentric and exhibit no effect from convective flows. The heat transport there is dominated by pure conduction. As  $\tau$  increases, however, isotherms behind the cylinder begin to grow in the downstream direction; the convection starts coming into play.

Another important objective in analyzing the present problem is to establish a general way to estimate the length of the transient period. Figure 2 shows that transient periods generally decrease with increasing Peclet numbers. This point can be argued more rigorously based on scale analysis [6]. Since the time required for fluid motion to reach a steady

state must be proportional to that for the fluid element to travel over a characteristic length with a characteristic velocity. Identifying that the length and the velocity scales are the radius of the cylinder and the free stream velocity, the above statement can be transformed to

$$\tau \sim Pe_{2a}^{-1}. \quad (10)$$

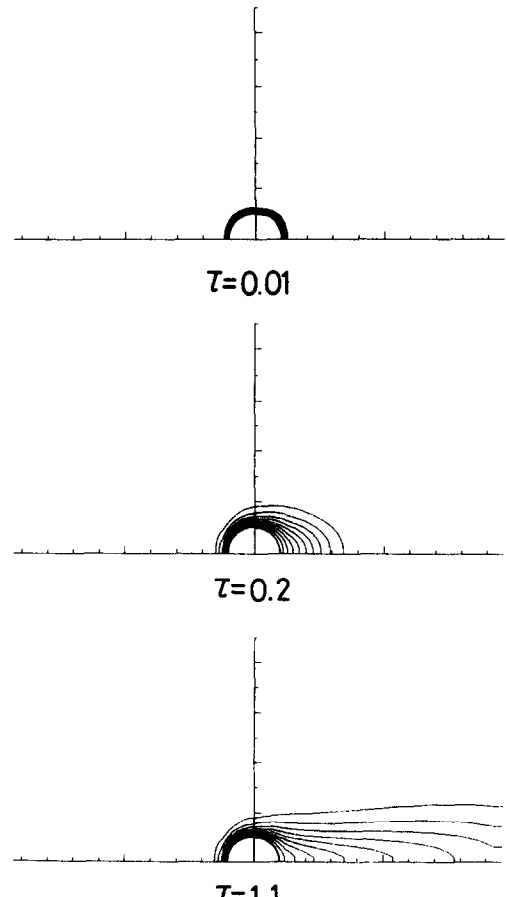


FIG. 3. Thermal layer growth about a circular cylinder at  $Pe_{2a} = 20$ . The contour interval is  $\Delta\theta = 0.1$ .

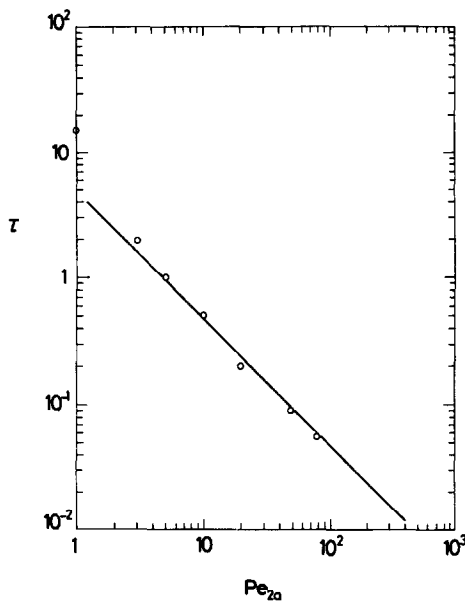


FIG. 4. Dimensionless time to reach steady states at different Peclet numbers.

Figure 4 shows dimensionless time to reach steady state as a function of Peclet number. The following equation is found to be a good fit in a range of  $3 \leq Pe_{2a} \leq 80$

$$\tau = \frac{5}{Pe_{2a}}. \quad (11)$$

Determining  $\tau$  at steady state is not easy. In the present study time-dependent Nusselt numbers are monitored in comparing with steady state ones that were numerically generated

neglecting the time derivative in the energy equation. Plotted values of  $\tau$  in the figure show the points at which the difference between the two becomes smaller than 5% in relative magnitude.

In summary transient heat transfer characteristics from a circular cylinder in a porous layer have been delineated when cross flows are present. The problem has been studied analytically and numerically. The major findings are:

- (1) heat transfer is dominated by pure conduction in the early stage of the transient process;
- (2) transition from pure conduction to convective state is smooth without any overshoot and undershoot in Nusselt number;
- (3) dimensionless time  $\tau$  to reach convective steady state is inversely proportional to Peclet number.

*Acknowledgement*—Computer time provided by the Agency of Industrial Science and Technology through its network (Research Information and Processing System) is gratefully acknowledged.

## REFERENCES

1. P. Cheng, Mixed convection about a horizontal cylinder and a sphere in a fluid-saturated porous medium, *Int. J. Heat Mass Transfer* **25**, 1245–1246 (1982).
2. S. Kimura, Forced convection heat transfer about an elliptic cylinder in a saturated porous medium, *Int. J. Heat Mass Transfer* **31**, 197–199 (1988).
3. H. Schlichting, *Boundary Layer Theory*. McGraw-Hill, New York (1968).
4. I. Pop and P. Cheng, The growth of a thermal layer in a porous medium adjacent to a suddenly heated semi-infinite horizontal surface, *Int. J. Heat Mass Transfer* **26**, 1574–1576 (1983).
5. H. S. Carslaw and J. C. Jaeger, *Conduction of Heat in Solids*. Clarendon Press, Oxford (1959).
6. A. Bejan, *Convection Heat Transfer*. Wiley, New York (1984).